Constitution and age hardening of Al–Sc alloys

N. BLAKE
Department of Metallurgical Engineering, Queen's University, Kingston, Ontario, Canada

M. A. HOPKINS
Department of Materials Engineering, Monash University, Clayton, Victoria, Australia

Aluminium-rich alloys from the Al–Sc system were examined to determine the form of the equilibrium phase diagram and to obtain information on age hardening of chill cast alloys. Samples containing up to 8.75 wt% Sc were examined using thermal analysis and optical microscopy. This work indicated a eutectic type of phase diagram with a eutectic temperature of about 665° C and a eutectic composition of about 0.6 wt% Sc. The scandium-rich primary phase was found to be $ScAl_3$ which is f c c with a lattice parameter of 0.4105 nm. Chill cast samples of a 1 wt% Sc alloy were examined for their age hardening behaviour over the temperature range of 225 to 360° C. A maximum hardness of 77 VHN was obtained after ageing at 250° C for 3 days. This hardness was retained after ageing for a total of at least 12 days. The hardening precipitates were $ScAl_3$ which were observed to form via a discontinuous precipitation mechanism. The $ScAl_3$ precipitates were observed to have a parallel orientation relationship with the matrix.

1. Introduction

The development of aluminium based age hardenable alloys for high temperature is generally limited by the non-equilibrium nature of the precipitates involved [1]. At high temperatures the precipitates, which may be coherent or semi-coherent, tend to transform to their equilibrium structure and lose coherency, which results in a decrease in hardness. One possible way around this problem is to use an alloying addition in which the precipitate is either coherent or semi-coherent in its equilibrium structure.

The most aluminium-rich compound in the Al–Sc system is $ScAl_3$, which has a face-centred cubic structure and a lattice parameter close to that of aluminium. The limited investigations of the aluminium-rich Al–Sc alloys [2–4] indicate that these alloys show promise for age hardenability. The information regarding the phase diagram for this area is limited and contradictory [5]. The present work was initiated to check on the nature of the phase diagram and to determine the age hardening behaviour of an Al–Sc alloy.

2. Experimental details

An Al–8.7 wt % Sc master alloy was made up by induction melting 99.99% aluminium and scandium with a purity of 99.9% in a recrystallized alumina crucible under an argon atomsphere. A series of alloys containing up to 5 wt % Sc was melted using the master alloy and either chill cast into a masssive copper mould or allowed to solidify slowly. Thermal analysis was carried out on these alloys to determine the eutectic temperature using a Perkin-Elmer DSC-2 at cooling and heating rates of 1.25 to 10° C min^{-1}. A series of slowly cooled cast alloys was examined using optical and scanning electron metallography, to determine the morphology of the primary phase. The structure and the lattice parameter of the primary $ScAl_3$

0022–2461/85 $03.00 + .12

particles was determined using a Philips X-ray diffractometer.

An Al–1 wt % Sc chill cast alloy was chosen for the investigation of age hardenability in this system. Samples of the alloy in the cast state were aged in oil baths at temperatures up to 360° C for times up to 450 h. Also a cast sample was cold rolled with 96% reduction and aged at 250° C for times of 3 and 100 h, and then overaged at 360° C for 18 h.

The microhardness of these samples was determined using a 500 g load. Thin foils for observation in the transmission electron microscope were prepared by electrothinning in a 40% acetic acid, 30% phosphoric acid, 20% nitric acid and 10% water solution. The foils were examined in either a JEOL 100C, Philips EM300 or EM420 electron microscope.

3. Results and discussion

3.1. Constitution

Thermal analysis in the heating mode indicated a thermal arrest at 655 ± 3° C which is about 5° C below the melting point of pure aluminium. This indicates a eutectic type of phase diagram which confirms the results of Drits *et al.* [2] who obtained a eutectic temperature of 655 ± 2° C. This is contrary to the work of Naumkin *et al.* [3] which indicated a peritectic reaction at 665° C. The other rare earths, i.e. yttrium, lanthanum, form eutectic systems with aluminium in contrast to the nearby transition elements (titanium, zirconium, hafnium) which form peritectic systems. However, the eutectic temperature at 665° C for scandium is higher than the other rare earth elements at about 640° C. Microstructural investigation of the slowly cooled alloy showed primary $ScAl_3$ particles in alloys with greater than 0.75 wt % Sc and none in a 0.6 wt % Sc alloy. From these observations the eutectic composition can be estimated to be approximately 0.6 wt % Sc which is in agreement with the work by Drits *et al.* [2].

3.2. Morphology and structure of primary $ScAl_3$

The primary particles of $ScAl_3$ in the slowly cooled alloys were highly faceted and had basically a cubic morphology, Fig. 1. In detail, the morphology was observed to be similar to a series of cubes radiating out and growing from the corners of a central cube. The highly faceted morphology indicates that $ScAl_3$ has a high α-factor as proposed by Jackson [6]. Jackson's analysis predicts that the atomic planes with a high density will be the slowest growing and therefore form facets. Thus, for a face-centred cubic structure the facet forming tendency should decrease in the order (1 1 1) > (1 0 0) > (1 1 0). However, the $ScAl_3$ with a cubic morphology would indicate (1 0 0) type facets. Highly faceted morphologies have also been observed in other trialuminide compounds, i.e. $TiAl_3$, $ZrAl_3$, $HfAl_3$, which have an ordered tetragonal structure [7].

The structure of extracted particles of primary $ScAl_3$ was determined by X-ray diffraction and found to be face-centred cubic with a lattice parameter of 0.4105 nm. This was also confirmed by transmission electron microscopy of the

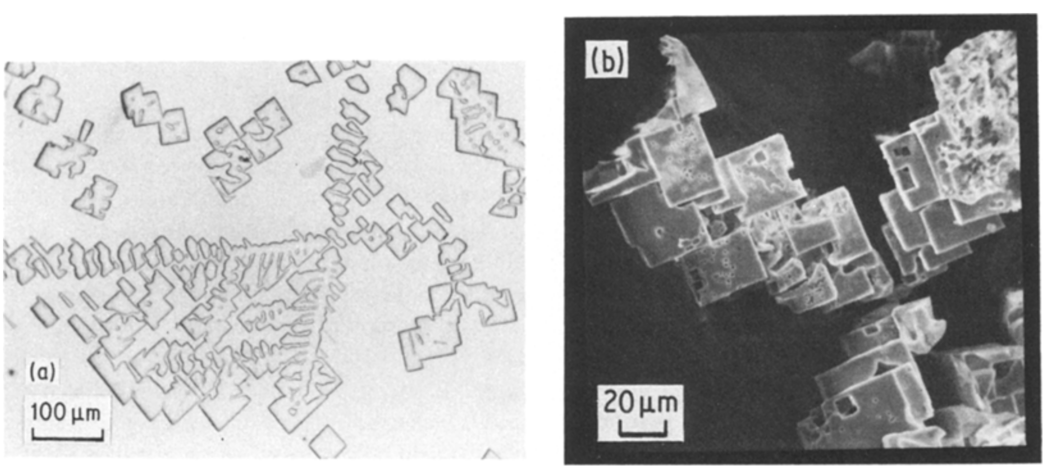

Figure 1 (a) Optical micrograph of primary $ScAl_3$ particle in slowly cooled master alloy. (b) Scanning electron micrograph of extracted $ScAl_3$ particle in slowly cooled master alloy.

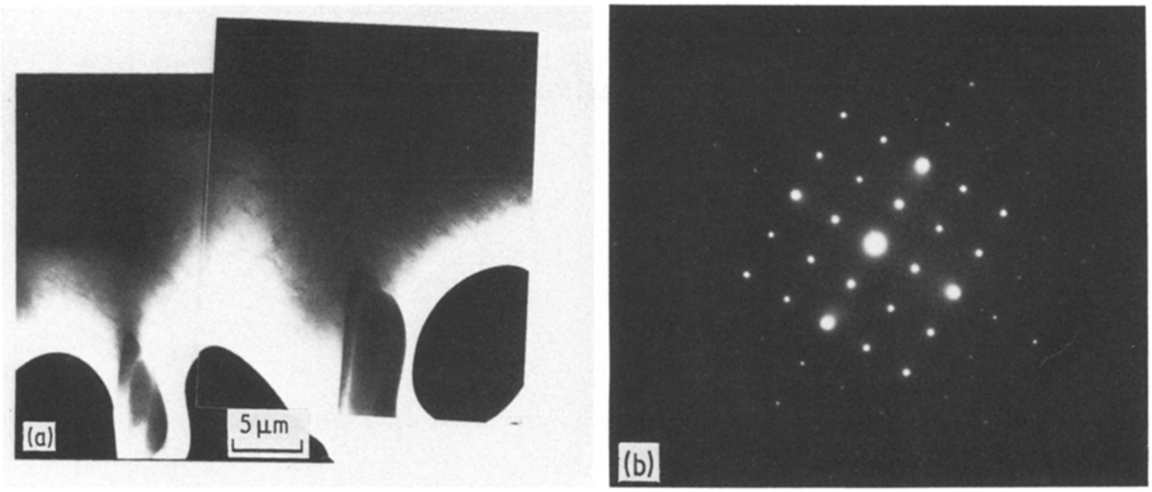

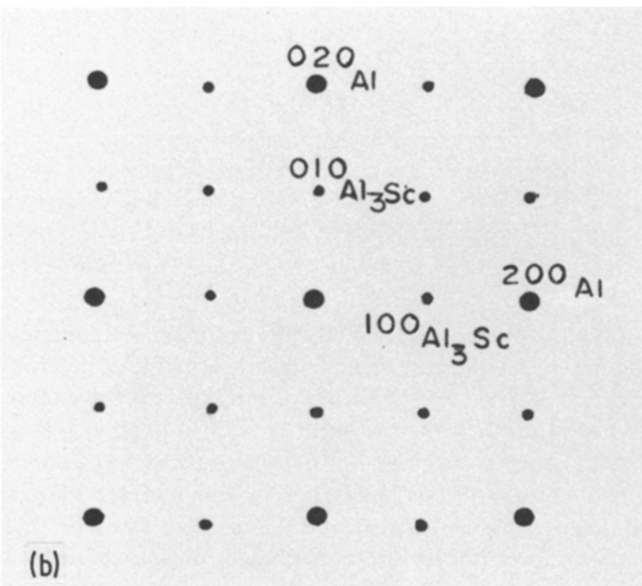

Figure 2 (a) Dark-field transmission electron micrograph of $ScAl_3$ particle in slowly cooled master alloy. (b) (0 0 1) orientation diffraction pattern from $ScAl_3$ particle.

master alloy which showed the $L1_2$ type structure, Fig. 2. This (0 0 1) orientation diffraction pattern shows the superlattice spots due to the ordered nature of the $L1_2$ structure.

3.3. Age hardening

A chill cast 1 wt % Sc alloy was aged at temperatures between 225 and 360° C and the microhardness/ageing curves are presented in Fig. 3. The as-cast alloy had a microhardness of 43 VHN. The time taken to reach maximum hardness decreased with increasing temperature. The maximum hardness obtained was 77 VHN after 3 days at 250° C and this hardness level was retained for a total of 12 days ageing when the test was terminated. Within the time limits of the tests only samples aged at 310 and 360°C showed a decrease of hardness with overageing. This indicates that the precipitates are fairly stable as would be expected from the fact that they are in their equilibrium state.

The age hardening process was followed using transmission electron microscopy for an alloy aged at 250° C. Samples were examined in the

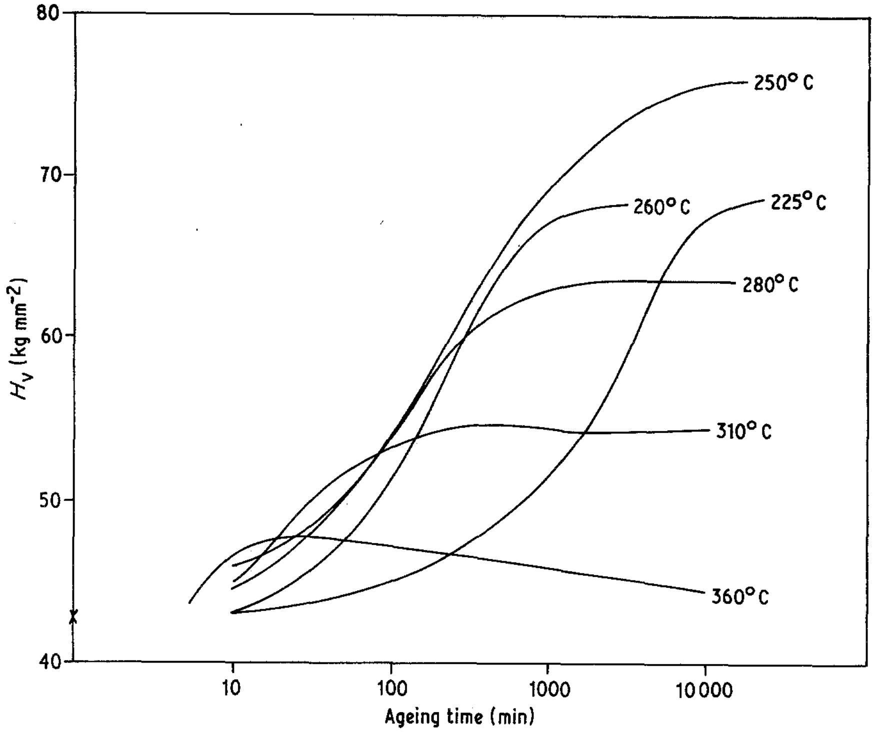

Figure 3 Ageing time/microhardness curves for an as-cast Al–1 wt % Sc alloy.

as-cast state, and aged for 3 or 100 h. One sample which had been aged for 100 h was then deliberately overaged by heating at 360° C for 18 h.

In the as-cast state, the structure consisted of fairly large grains of the aluminium matrix, some of which contain a limited number of rod-shaped precipitates of $ScAl_3$. These precipitates may have been formed during the cooling after chill casting or on ageing at room temperature.

In the samples aged for 3 and 100 h a large number of rod-shaped, dendritic or spherical precipitates were evident, Fig. 4. The rod-shaped and dendritic precipitates were predominant and had a width of < 30 nm and a separation of 0.2 to 0.1 μm. It was difficult to discern a quantitative difference in the number of precipitates between the 3 and 100 h samples. The precipitates were arranged in fan-shaped or cellular arrays and often the edge of this array was associated with a grain boundary. The

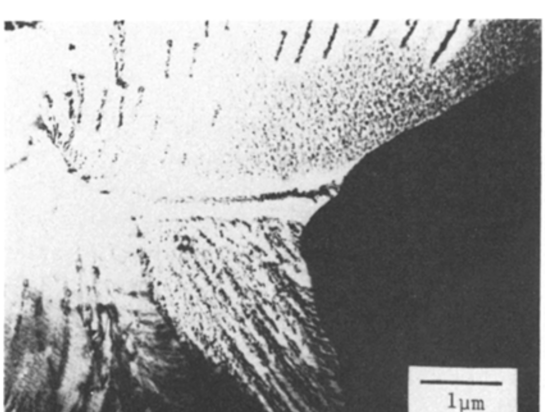

Figure 4 Transmission electron micrograph of $ScAl_3$ precipitates after ageing for 3 h at 250° C.

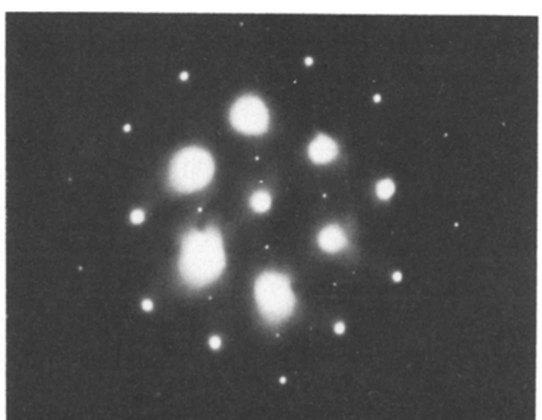

Figure 5 SADP from precipitates and matrix which shows parallel orientation relationship. (0 1 1) orientation.

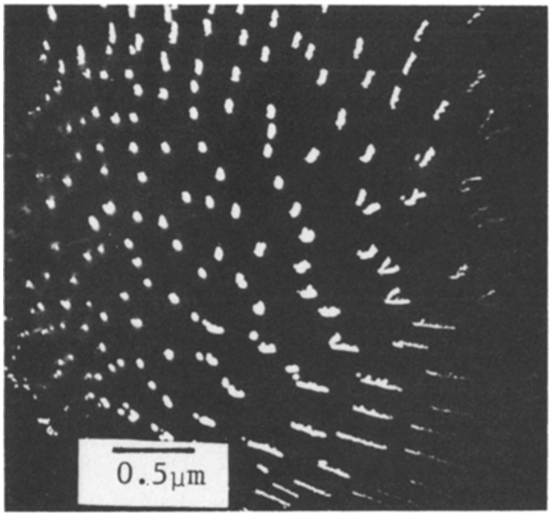

Figure 6 Dark-field transmission electron micrograph of $ScAl_3$ precipitates in an aged alloy. From superlattice diffraction spot.

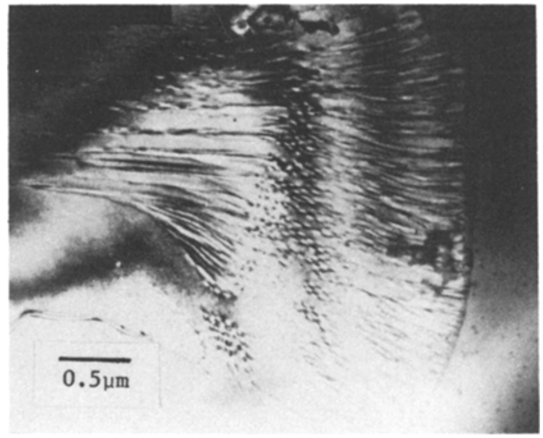

Figure 8 $ScAl_3$ precipitates arranged in a fan-shaped pattern.

precipitates were only evident in the microscope at certain tilts and superlattice spots could often be observed on the diffraction pattern in these orientations. The precipitates were observed to have a parallel orientation relationship with the matrix, Fig. 5. Close examination showed a variety of structures in the precipitates, such as the spherical or branched dendritic nature of some precipitates, Fig. 6, or the rod-shaped precipitates which appeared to be broken up into short segments, Fig. 7. This latter observation is probably due to some form of contrast effect.

These precipitates were exactly analogous to those found in aged chill cast Al–Zr [8–11] and Al–Hf [12] alloys. The mechanism of precipitation of the rod and dendritic structures in these aluminium transition metal alloys is one of discontinuous precipitation where the supersaturated solid solution decomposes into precipitate and matrix behind an advancing grain boundary. In the Al–Zr and Al–Hf alloys a metastable $L1_2$ structure precipitate forms initially, but on further ageing this breaks down to the equilibrium tetragonal structure. In these alloys also the metastable trialuminide precipitates have a lattice parameter very close to that of aluminium and have a parallel orientation relationship with the matrix.

Many of the features observed in these alloys were also found in the Al–Sc aged alloys. The rod-shaped and dendritic precipitates often seemed to branch out and form a fan-shaped pattern, Fig. 8. Protrusion of the precipitates at the grain boundaries often generated an uneven boundary, Fig. 9. This indicates that the

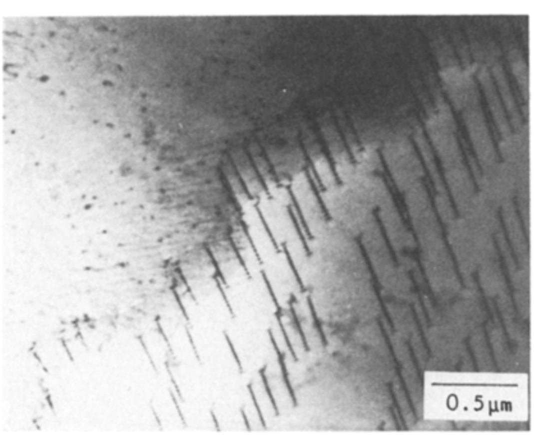

Figure 7 Bright-field transmission electron micrograph showing rod-shaped precipitates.

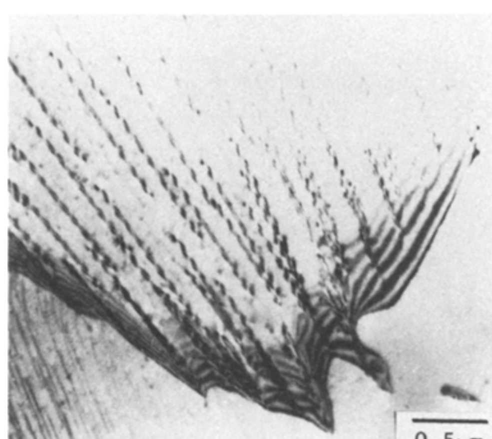

Figure 9 $ScAl_3$ precipitates protruding into an advancing grain boundary.

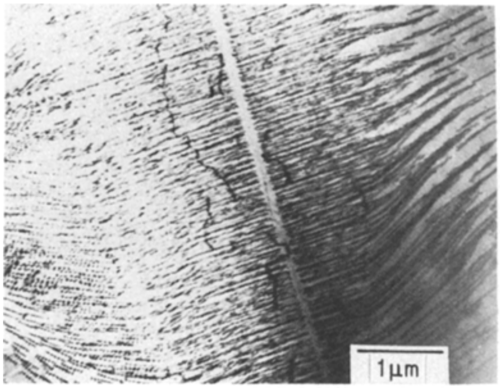

Figure 10 $ScAl_3$ precipitates in a single grain which have grown towards each other.

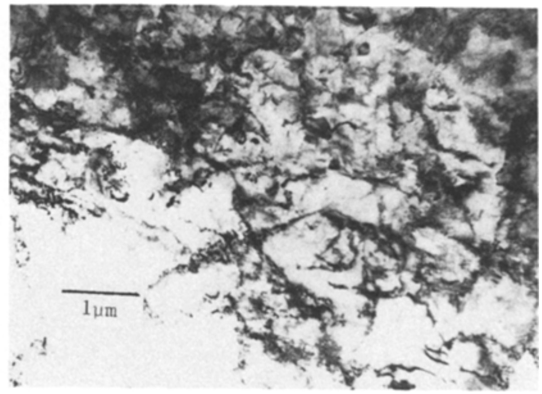

Figure 12 Transmission electron micrograph of cold rolled Al–1 wt % Sc alloy.

precipitates were providing some of the driving force for the migration of the boundary. The structure shown in Fig. 10, indicates the growth of some precipitates towards each other in a single grain. This can be explained as the result of a segment of the original grain boundary moving in the opposite direction to the adjacent segments and the precipitates then fanning out behind this segment and meeting each other at a 180° angle, Fig. 11 [10].

The sample which had been deliberately overaged showed a decrease in hardness of 13 VHN from the maximum condition. The uniformity of the precipitate structure appeared to have been degraded and some grain growth had occurred.

The cold rolled alloys showed a faster age hardening response with an increase in hardness from 58 VHN in the cold rolled state to 81 VHN after ageing for 3 h at 250° C. The 100 h specimen showed a degree of hardness to 63 VHN and this dropped to 57 VHN after the final overageing treatment. The structure associated with this treatment showed a dislocation network in the cold rolled state with no precipitates present, Fig. 12. After 3 h ageing the structure had recrystallized and some precipitates had formed, but not in the fan-shaped arrays as found in the as-cast alloys. The precipitates were equiaxed or elongated and were often situated within the grains or at the grain boundaries, which they pinned, Fig. 13. Dark-field images often showed a number of precipitate particles at the same orientation within a single grain. The grain size in this ageing state was between 0.4 and 0.7 µm. An increase in grain size to approximately 1.0 µm occurred after ageing for 100 h, but the precipitates remained the same size. On overageing, the grain size increased to 1.5 µm and larger. Less of the smaller sized precipitates were also observed, Fig. 14.

After cold rolling the precipitation was not via

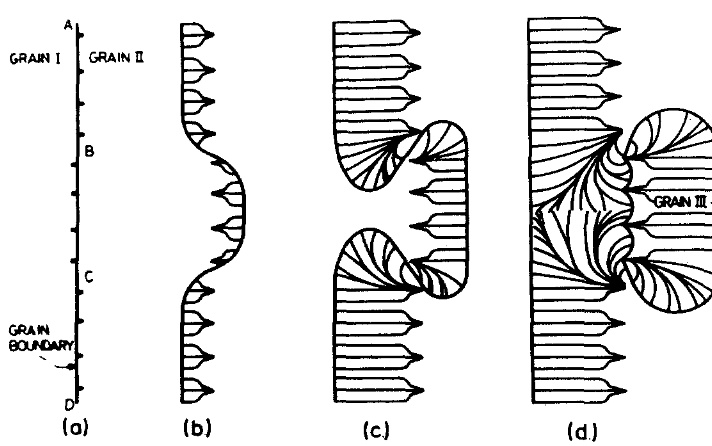

Figure 11 Schematic diagram of the development of the precipitate arrangement in Fig. 10. (After Nes and Billdal [10].)

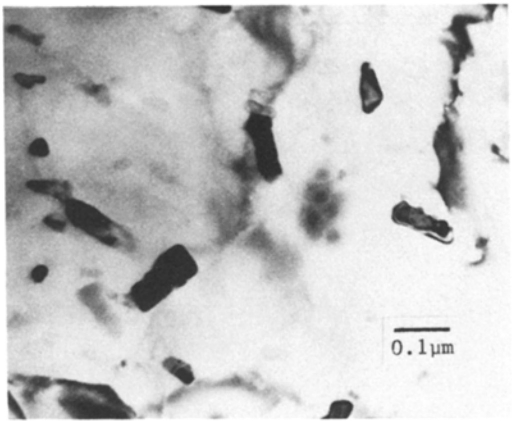

Figure 13 Transmission electron micrograph of $ScAl_3$ precipitates in a cold rolled alloy aged for 3 h at 250° C.

the discontinuous mechanism as in the as-cast alloy. The $ScAl_3$ precipitates were effective at pinning the grain boundaries and thus maintained a fine grain size. The dislocation networks resulting from cold deformation provided a more favourable site for nucleation and growth of the $ScAl_3$ precipitates.

4. Conclusions

1. The aluminium-rich end of the Al–Sc system has a eutectic reaction at 655° C at 0.6 wt % Sc between α-Al and $ScAl_3$.

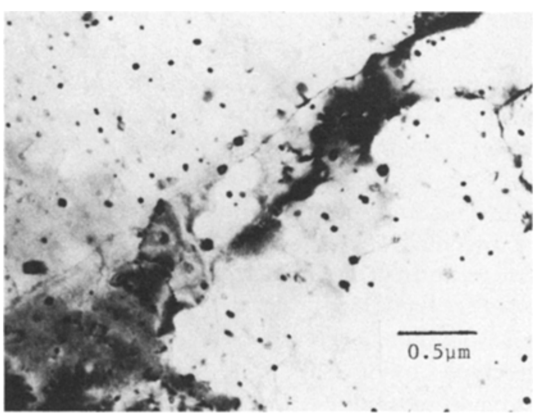

Figure 14 Transmission electron micrograph of the structure of an overaged cold rolled alloy.

2. $ScAl_3$ has an $L1_2$ type structure with a lattice parameter of 0.4105 nm. This phase grows with a faceted solid/liquid interface and has basically a complex cubic morphology.
3. Chill cast Al–1 wt % Sc alloys are age hardenable with the super-saturated aluminium matrix decomposing to aluminium with $ScAl_3$ precipitates via a discontinuous precipitation mechanism.
4. The ageing of a cold rolled chill cast Al–1 wt % Sc alloy at 250° C results in precipitation of $ScAl_3$ particles both within the grains and at grain boundaries.

Acknowledgement
The authors would like to acknowledge the assistance of Dr B. Muddle with some of the electron microscopy.

References

1. C. M. ADAM, "Rapidly Solidified Amorphous and Crystalline Alloys", edited by B. H. Kear, B. C. Geissen and M. Cohen (Elsevier, 1982) p. 411.
2. M. E. DRITS, E. J. KADANER, T. V. DOBATKINA and N. I. TURKINA, *Russian Metallurgy* (4) (1973) 152.
3. O. P. NAUMKIN, V. T. TEREKHOVA and E. M. SAVITSKII, *ibid.* (4) (1965) 128.
4. M. E. DRITS, L. S. TOROPOVA, YU. G. BYKOV, L. B. BER and S. G. PAVLENKO, *ibid.* (1) (1982) 148.
5. R. P. ELLIOT and F. A. SHUNK, *Bull. Alloy Phase Diagram* **2** (1981) 222.
6. K. A. JACKSON, *J. Crystal Growth* **1** (1967) 1.
7. N. W. BLAKE, PhD thesis, Queen's University, Kingston, Canada (1982).
8. N. RYUM, *Acta Metall.* **17** (1969) 269.
9. E. SAHIN and H. JONES, "Rapidly Quenched Materials III" (Metals Society, London, 1978) p. 138.
10. E. NES and H. BILLDAL, *Acta Metall.* **25** (1977) 1039.
11. O. IZUMI and D. OESCHLAGEL, *Scripta Metall.* **3** (1969) 619.
12. N. RYUM, *J. Mater. Sci.* **10** (1975) 2075.

Received 29 August
and accepted 13 September 1984